TITLE: High-throughput isolation and culture of human gut bacteria with droplet microfluidics

AUTHORS: Max M Villa[†‡^], Rachael J Bloom[*‡^], Justin D Silverman[§||‡], Heather K Durand[†‡], Sharon Jiang[†‡], Anchi Wu[°], Shuqiang Huang[‡°**], Lingchong You[‡°], and Lawrence A David[†‡§°]

AUTHOR AFFILIATIONS:

*University Program in Genetics and Genomics, Duke University, Durham, NC, 27708
† Department of Molecular Genetics and Microbiology, Duke University, Durham, NC 27708
‡ Center for Genomic and Computational Biology, Duke University, Durham, NC 27708
§ Program in Computational Biology and Bioinformatics, Duke University, Durham, NC 27708
|| Medical Scientist Training Program, Duke University, Durham, NC 27708
° Department of Biomedical Engineering, Duke University, Durham, NC 27708
**Institute of Synthetic Biology, Shenzhen Institutes of Advanced Technology, Chinese Academy of Sciences, Shenzhen 518055, People's Republic of China

^ denotes equal first-authorship

CORRESPONDING AUTHOR:

Lawrence A David
CIEMAS, Room 2171
101 Science Drive, Box 3382
Durham, NC 27708
919-668-5388
lawrence.david@duke.edu

Abstract

Isolation and culture of gut bacteria enable testing for microbial roles in disease and may also lead to novel therapeutics. However, the diversity of human gut microbial communities (microbiota) impedes comprehensive experimental studies of individual bacterial taxa. Here, we combine advances in droplet microfluidics and high-throughput DNA sequencing to develop a platform for isolating and assaying microbiota members in picoliter droplets (MicDrop). MicDrop can be used to create millions of distinct bacterial colonies in a single experiment while using off-the-shelf parts compact enough to fit in an anaerobic chamber. In proof-of-concept experiments, we used the platform to characterize inter-individual metabolic variation among hundreds of polysaccharide-degrading gut bacteria from nine stool donors. We also used MicDrop to test the hypothesis that growth kinetics of individual gut bacterial taxa are associated with long-term community dynamics in an artificial gut. These demonstrations suggest the MicDrop platform could support future diagnostic efforts to personalize microbiota-directed therapies, as well as to provide comprehensive new insights into the ecology of human gut microbiota.

Introduction

Bacterial culture was among the first techniques used to study human gut microbiota[1]. Bacterial isolation efforts beginning in the early 1900s identified key enteric genera such as *Bacteroides, Bifidobacterium*, and *Bacillus*[2]. Microbes isolated since then have served as crucial reagents for experiments. Gut bacterial isolates allow testing causal roles for specific microbes in animal models of metabolic and auto-immune disorders[3-5]. Bacterial isolates can also be genetically modified and tested *in vitro* to identify enzymatic machinery in processes like the fermentation of dietary fiber[6], and cocktails of cultured bacteria are being explored as therapeutics for *C. difficile* infections and cancer[7-9].

Yet a key challenge for current microbiota culturing efforts has been keeping pace with increasing knowledge and interest in gut microbial diversity. Culture-independent methods based on high-throughput 16S rRNA sequencing have revealed the average individual harbors hundreds of distinct enteric bacterial strains[10-13]. Moreover, unrelated individuals likely share no more than ~30% of bacterial strains[14]. Prevailing culture techniques do not scale to the diversity of microbes spanning human populations. Because most taxa are rare, exhaustive capture of bacterial species from even a single stool sample requires laborious spotting of thousands of bacterial colonies[15,16]. To reduce the human effort needed for such experiments, state-of-the-art culture assays leverage plate and liquid handling robots; but, even these automated efforts tend to be limited to tens of strains[17,18]. This limitation stems in part from the physical constraints of typical plate-based culture methods, which grow bacteria in wells ranging from centimeters to millimeters in diameter. Even relying on 96- and 384-well

plates, conventional large-scale culture efforts may require loading and handling dozens of plates under anaerobic conditions[18].

An alternative approach is to culture bacteria in small volumes (nano- to pico-liters) by separating microbes into microscale wells. Devices composed of thousands of such wells have been used to culture both lab strains of bacteria and fungi[19], as well as isolate previously uncultured bacteria from the gut and soil[20,21]. Even higher-throughput experiments are possible by compartmentalizing microbes in droplets of media that are tens to hundreds of microns in diameter and separated by immiscible oils and engineered surfactants[22,23]. Because droplets are not limited by the need to microfabricate physical wells or channels, millions of distinct culture volumes can be created on the order of minutes. Droplet techniques have so far been used to isolate uncultured microbes from seawater and soil communities[20,24,25], assess microbial cross-feeding[26], track population dynamics of individual bacteria[27], and examine antibiotic sensitivity and commensal-pathogen interactions of human gut and oral microbiota[28,29]. Still, existing droplet microfluidic approaches for assaying bacteria have required combining complex emulsion techniques (water-oil-water) with flow cytometers or custom on-chip droplet sorting devices. These protocol requirements limit the accessibility of droplet technologies for bacterial assays and in their present form require equipment that does not fit into typical anaerobic chambers, which are needed to culture human gut bacteria[30].

Here, we developed a platform to isolate and culture bacteria from human gut microbiota in droplets (MicDrop) using accessible techniques and equipment. A key challenge our method addresses is how to measure the growth of isolates within distinct

92 microfluidic droplets. To accomplish this, we rely on 16S rRNA as intrinsic DNA
93 barcodes that are shared between droplets carrying the same bacterial taxa, which we
94 refer to here as a sequence variant or SV[31]. This approach in turn allows us to measure
95 isolate growth in droplets without the need for double-emulsion techniques or droplet
96 sorting. Instead, we combine single-emulsion (water-in-oil) microfluidic droplet protocols
97 with molecular techniques (qPCR and 16S rRNA sequencing). These simplified
98 protocols allow us to employ off-the-shelf microfluidic pumps and chips, which are
99 compact enough to fit within typical anaerobic chambers. Using MicDrop, we
100 characterized dietary polysaccharide metabolism among hundreds of gut bacteria from
101 nine individuals. We then employed MicDrop to generate growth curves for dozens of
102 distinct SVs in a single experiment, which we in turn used to investigate long-term
103 microbiota dynamics of an artificial human gut. Together, these findings showcase the
104 potential for microfluidic droplet techniques to characterize the growth and function of
105 individual bacterial strains from complex gut microbial communities in high-throughput.
106
107

Results

MicDrop: a platform for culturing human gut microbiota in droplets

To isolate and culture individual gut bacteria from human gut microbiota, we merged concepts from prior microfluidic droplet protocols with high-throughput DNA sequencing (Fig. 1; Experimental Procedures). Our protocol first randomly encapsulates individual bacterial cells from gut microbiota into picoliter-sized droplets (Fig. 1A). Gut microbiota samples are diluted before encapsulation using the Poisson distribution at a loading concentration that optimizes the number of droplets loaded with cells (~10-26%) against the number of droplets loaded with more than one microbe (~95-86% of loaded droplets contain single cells) (Supplementary Fig. 1)[32]. Since many gut bacteria are obligate anaerobes, encapsulation takes place in an anaerobic chamber and droplets are subsequently incubated under anaerobic conditions (Supplementary Fig. 2). To track SV growth, we can avoid having to identify and sort bacteria by assuming that droplets are either empty or loaded with clonal isolates whose progeny share the same 16S ribosomal rRNA (rRNA) sequence, meaning genomic material accumulating across all droplets reflects the growth of SVs grown in isolation (Fig. 1A-D). We therefore track isolate growth in droplets at a given time point using bulk bacterial DNA extraction without droplet sorting, followed by DNA sequencing and total quantification (qPCR) of 16S rRNA. The product of relative SV levels from 16S rRNA sequencing and total 16S rRNA levels yields an estimate of the absolute levels of each SV across all droplets at the time of sampling.

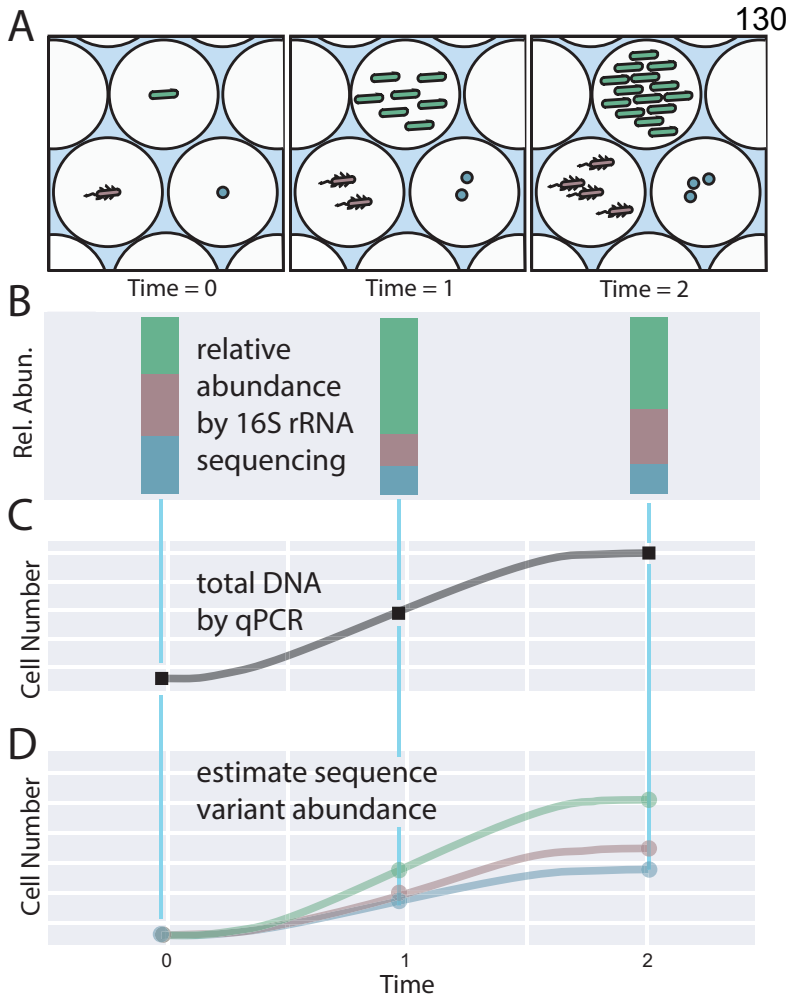

Figure 1. MicDrop concept (A) Schematic of bacterial loading and growth in droplets over time. Bulk DNA is collected across all droplets and (B) the 16S rRNA gene is sequenced to establish the relative abundance of each sequence variant. (C) qPCR is used on the same samples to estimate the total abundance of all bacteria. Relative abundances are then multiplied by total bacterial levels to estimate sequence variant abundances (D).

To explore the feasibility of the MicDrop platform, we initially examined bacterial replication and isolation in droplets, as well as the use of DNA sequencing to track bacterial levels. We found aerobic monocultures of fluorescent *Escherichia coli* replicated in droplets in a qualitative manner that resembled growth on conventional Petri dishes (Supplementary Fig. 3). Droplet stability experiments suggested that

bacteria could be studied in droplets for at least 5 days (Supplementary Fig. 4). Next, microscopy showed droplets could be used to segregate clonal isolate populations with distinct morphology and motility out of mixed microbial communities (Supplementary Fig. 5). Human fecal microbiota isolated and cultured in droplets exhibited 2.6 times more diversity than when grown in mixed conditions (Supplementary Fig. 6), which is consistent with the hypothesis that droplet isolation enables slow-growing microbes to be sheltered from competition with fast-growing bacteria[20]. Last, we found DNA-based techniques could be used to track bacterial levels in droplets. Quantitative growth measurements using qPCR of the 16S rRNA gene sampled every two hours from liquid cultures were also similar to *E. coli* grown on plates (ρ=0.95, p=8.7e-9; Spearman correlation; Supplementary Fig. 7). Next, using DNA sequencing, we analyzed a mixture of 10 bacterial strains that were isolated using MicDrop and grown under varying antibiotic conditions for 24 hours. We found that resulting bacterial DNA levels in droplets corresponded to isolates' optical densities in reference well-plates (accuracy=75%; Supplementary Fig. 8).

A droplet assay for prebiotic consumption by human gut microbes

To demonstrate how MicDrop could be applied to problems in human gut microbiology, we used the platform to measure bacterial utilization of carbohydrates. In typical carbohydrate utilization screens, bacteria are cultured in defined media containing a carbohydrate as the sole carbon source[17,33]. Microbes that replicate are assumed to be capable of utilizing the carbohydrate and are termed "primary degraders"[34,35]. The biology of primary degraders is of increasing interest because bacterial metabolism of

168 select indigestible carbohydrates (prebiotics) leads to the growth and activity of gut
169 microbes with multiple beneficial impacts on host health[17,36-40]. Still, bacterial prebiotic
170 metabolism is incompletely understood, particularly with regards to the origins of wide
171 inter-individual variation in microbiota metabolic potential[41-43].

172 To explore how the MicDrop platform could assay bacterial prebiotic metabolism
173 (Fig. 2A), we first loaded a previously characterized type strain *Bacteroides*
174 *thetaiotaomicron* ATCC 29148 into microfluidic droplets and standard 96-well plates.
175 Consistent with both prior studies[17] and our well-plate experiments, *B. thetaiotaomicron*
176 ATCC 29148 replicated in droplets on pullulan and levan, but not on lamanarin or a no
177 carbohydrate control (Fig. 2B). We next tested how the MicDrop prebiotic assay
178 performed using artificial microbial communities assembled from seven human gut
179 isolates (Fig. 2E). Using 96-well plate experiments as our reference (Fig. 2C & 2D,
180 Supplementary Fig. 9), we found the sensitivity, specificity, and false discovery rate of
181 the MicDrop prebiotic assay to be 80%, 93%, and 9%, respectively (Supplementary
182 Table 1). Finally, to assess the reproducibility of the MicDrop prebiotic assay, we used
183 the same frozen fecal sample to compare the results of two separate experimental
184 sessions. We observed higher correlation between replicates from the same session
185 (ρ= 0.73-0.78, p<0.0001, Spearman correlation) than between replicates across
186 sessions (ρ=0.57, p=1.67e-17, Spearman correlation). One explanation for the
187 difference in correlation is that microbial communities re-assembled in different
188 configurations each time microbiota was revived from frozen stool[44]. Indeed, controlling
189 for microbiota differences between droplet inocula elevated the between session
190 correlation (ρ=0.74, p=5.14e-19, Spearman correlation, Fig. 2F).

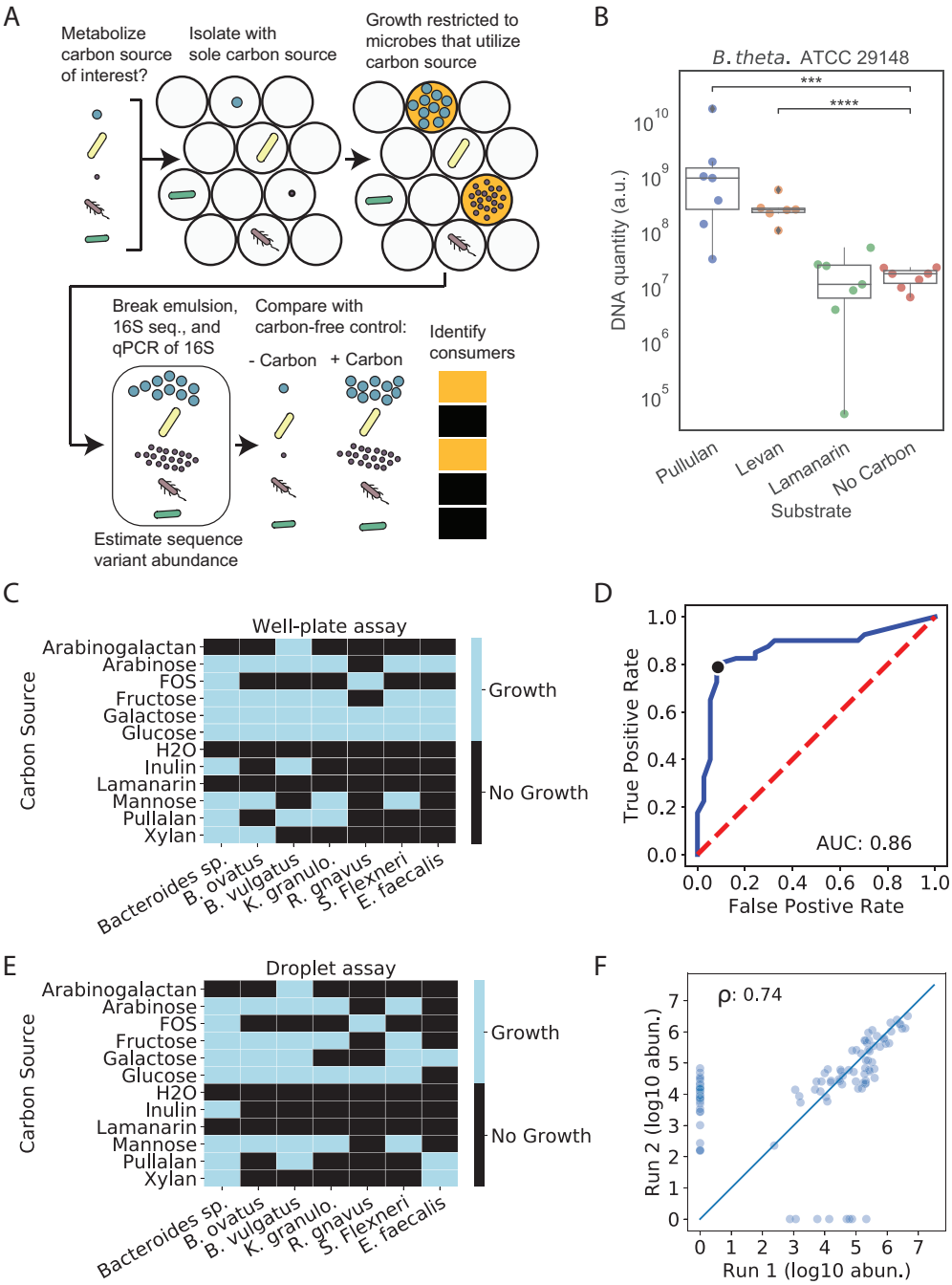

Figure 2. A prebiotic utilization screen based on the MicDrop platform
(A) Schematic of MicDrop prebiotic assay. (B) Droplet monoculture growth of *B. thetaiotaomicron* in microfluidic droplets measured by qPCR. (C) Results of 96-well plate growth of gut bacterial isolates across 11 carbohydrates. (D) ROC curve of MicDrop assay results at different growth threshold cut-offs using (C) as a reference. The black dot indicates the growth threshold that maximizes the true positive rate while minimizing the false positive rate, depicted in (E). (F) Correlation between two different MicDrop sessions (each carried out in triplicate) on the same frozen fecal sample and five different carbohydrates. Points indicate median growth of different SVs across each experimental session.

Identifying primary degraders from human guts across multiple prebiotics

We next applied the MicDrop prebiotic assay to microbiota from nine healthy human stool donors. We assayed growth on three consumer-grade prebiotics (inulin, galacto-oligosaccharides (GOS), and dextrin) and a lab-grade prebiotic (xylan). Out of the 588 SVs detected across donor stool samples, MicDrop identified a total of 285 primary degraders that grew on at least one of the screened prebiotics (Fig. 3A). Prebiotic utilization patterns of primary degraders were similar to those of matched bacterial strains in a reference database of microbial carbohydrate utilization[45,46]. Among the instances when matched bacteria were annotated as consuming a prebiotic in the database, 86% were detected by MicDrop (p<0.001; permutation test). Still, we did find that 52% of instances when MicDrop indicated a primary degrader to consume a prebiotic were not reported for matched bacteria in the database (p=0.34; permutation test), which may in part reflect incomplete enumeration of bacterial carbohydrate utilization in the reference.

We next explored the hypothesis that differences in the presence or absence of primary degraders could drive inter-individual variation in human prebiotic response. Evidence arguing against this hypothesis included observing that multiple SVs capable of growing on the tested prebiotics were present in all subjects (median: 12.5 ± 6.1); Fig. 3B, Supplementary Table 2). Additionally, primary degraders were more likely to be shared between individuals than SVs not identified as primary degraders in stool samples (p=0.00122, Chi-square test). Concordant with human studies showing that even individuals with low prebiotic fermentation *in vivo* exhibit at least some prebiotic

fermentative capacity *in vitro*[35], our findings support the hypothesis that primary degraders are found across most individuals.

Still, we also found evidence for inter-individual variation in primary degrader composition and abundance. We observed differences in the richness of primary degraders across subjects (p<0.001, Two-way ANOVA; Fig. 3B). We also found subject identity explained more variation (R^2=0.30, PERMANOVA; Supplementary Table 3) than prebiotic type (R^2=0.16, PERMANOVA; Supplementary Table 3) in overall primary degrader growth. Last, we observed differences in the relative abundance of primary degraders in inoculating fecal communities (p<0.0001, Two-way ANOVA; Fig. 3C). Thus, while primary degraders are likely present in most individuals, differences in polysaccharide metabolism may be due to inter-individual variation in primary degrader abundance in the gut[41,42].

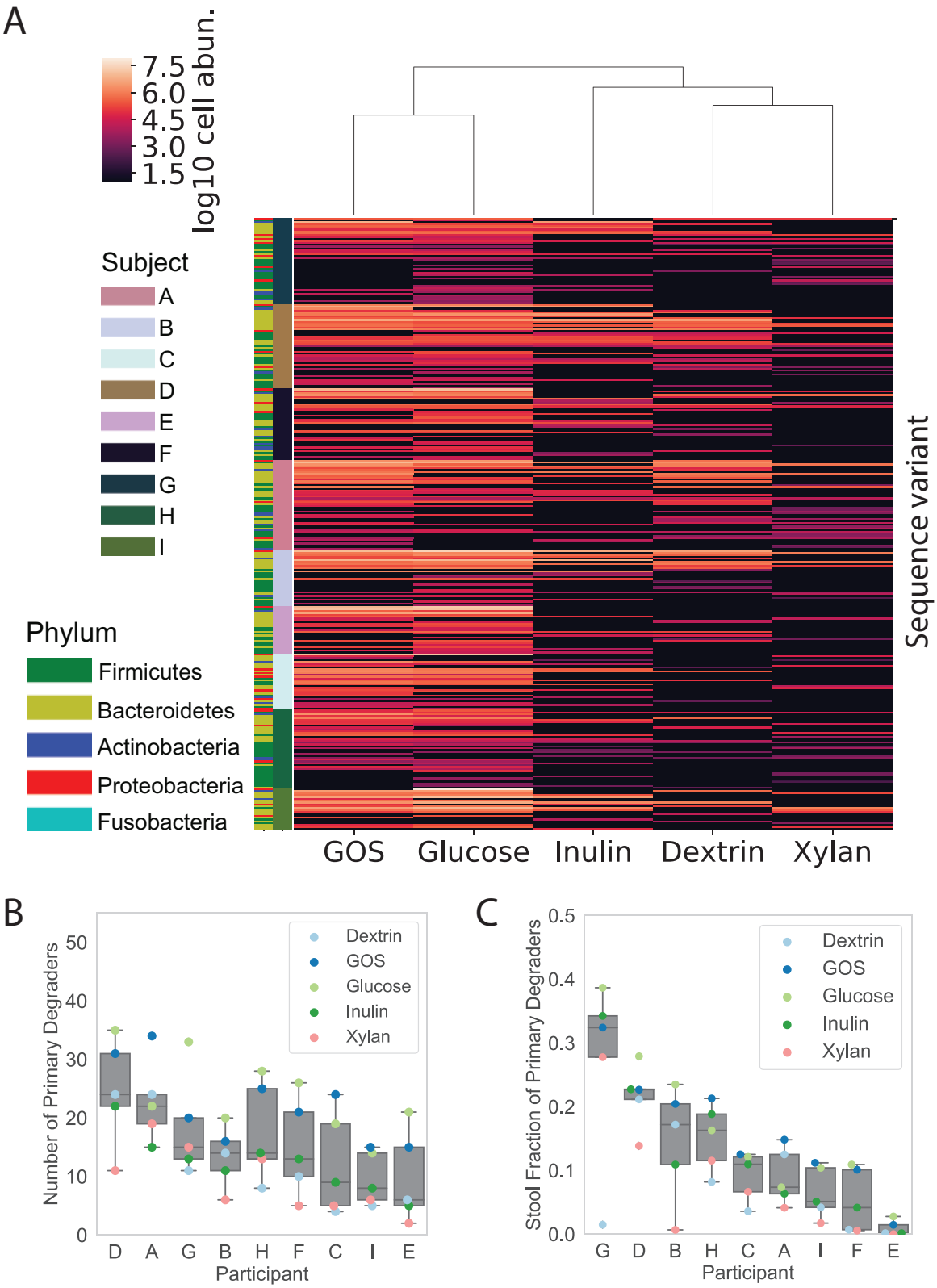

Figure 3. **MicDrop prebiotic assay carried out on fecal samples from nine individuals.** (A) Microbial carbohydrate preferences for 328 SVs from nine healthy human donors. Of these SVs, 285 grew on at least one of the prebiotics (*i.e.* GOS,

inulin, dextrin, or xylan). (B) The number of primary degraders detected by MicDrop and (C) the relative abundance of primary degraders in stool samples differed by participant and prebiotic ($p<0.001$, Two-way ANOVA). Participant orderings in (B) and (C) are sorted by median values.

High-throughput estimation of growth dynamics of human gut microbiota

In a second set of demonstration experiments, we used the MicDrop platform to explore the dynamics of human gut microbiota in artificial gut systems. Such systems have been used when *in vivo* microbiota research is challenging, including measuring the effects of nutrition on the infant gut, systematic antibiotic testing, and investigating chemotherapy-induced dysbioses[47,48,49]. Still, a recurring challenge of artificial gut models has been their inability to completely reconstruct *in vivo* microbial communities. After inoculation, these models often decrease in diversity within 24 hours[50-52], and as little as 15% of the starting community may ultimately remain after a week of culture[53]. A potential explanation for part of this diversity loss is that bacteria are sensitive to media conditions: studies using individual gut bacterial strains show growth can be affected by even a single medium component[54]; and, varying media used in artificial guts leads to broad scale changes in microbial community structure[55,56]. Still, the hypothesis that individual gut microbes' suitability to media is associated with their long-term persistence in artificial gut models has not been fully explored, likely due in part to the challenges of isolating and assaying each component species in these communities.

To test the hypothesis that growth of individual microbial SVs in a particular medium would correspond to SV persistence in an artificial gut setting, we used stool from a healthy human donor to inoculate a continuous flow bioreactor system we have used in past gut microbial ecology studies[57,58]. The artificial gut was supplied with

266 modified Gifu Anaerobic Medium (mGAM)[59], which features a variety of carbon and
267 nitrogen sources, as well as extra amino acids, vitamin K, and hemin. We chose mGAM
268 because it enables a wide growth of mammalian gut bacteria[54,59]. Yet, despite this
269 choice of medium, microbiota dynamics in the artificial gut exhibited the same loss in
270 diversity observed in prior studies (Supplementary Fig. 10)[50,53]. At the end of two weeks
271 of culture, only 23% and 18% of inoculating bacteria genera and SVs, respectively,
272 were still detected in the artificial gut (Supplementary Table 4).

273 A fresh stool sample from the same donor used to inoculate the artificial gut was
274 then assayed by the MicDrop platform. To additionally demonstrate the potential for
275 MicDrop to assess the kinetics of bacterial growth over time, we created replicate
276 droplet populations and destructively sampled them at hourly intervals for the first 24
277 hours, and daily for four subsequent days after inoculation. Among the resulting time
278 series, 94 SVs were detectable in droplets, meaning they appeared in >5 time points;
279 Table 1, Supplementary Fig. 11). These SVs included representatives from the major
280 human gut bacterial phyla (the Actinobacteria, Bacteroidetes, Firmicutes, and
281 Proteobacteria) and represented 76% of the inoculum's SVs, a proportion approaching
282 prior culture efforts using mGAM medium[59]. Of the detectable SVs, we then measured
283 how many exhibited evidence for growth in droplets. We defined a cut-off for growth as
284 inferred doublings of at least 2.14 times (Δ ln(SV DNA abundance) $\geq$ 1.48) based on our
285 antibiotic-based control experiments (Supplementary Fig. 8). A total of 34 SVs were
286 defined as growing (Fig. 4A), which accounted for 25% of the inoculum's SVs. Of the
287 SVs with positive growth, 12 SVs were not detected by sequencing in the inoculum,
288 which suggests they could be laboratory contaminants. Still, these SVs resemble known

289 gut bacteria (Supplementary Table 5) and may alternatively represent rare microbes

290 that require culture to be detected, which is a previously reported phenomenon[60].

291 **Table 1.** Number and fraction of microbes from a human stool sample cultured by
292 MicDrop in mGAM medium. SVs were considered as 'detected' if present in more than
293 five longitudinal measurement. 'Growth' was defined by an inferred number of doublings
294 equal or greater than 2.14.
295

Taxonomic level	Taxa in inoculum	Taxa detected in droplets	Taxa in inoculum & detected in droplets	Fraction of inoculum detected in droplets	Taxa grew in droplets	Taxa in inoculum & grew in droplets	Fraction of inoculum that grew in droplets
Phylum	4	5	4	1.00	5	4	1.00
Class	10	11	10	1.00	7	5	0.50
Order	10	14	10	1.00	8	5	0.50
Family	17	21	16	0.94	13	7	0.41
Genus	56	53	40	0.71	20	13	0.23
Sequence Variant	89	94	68	0.76	34	22	0.25

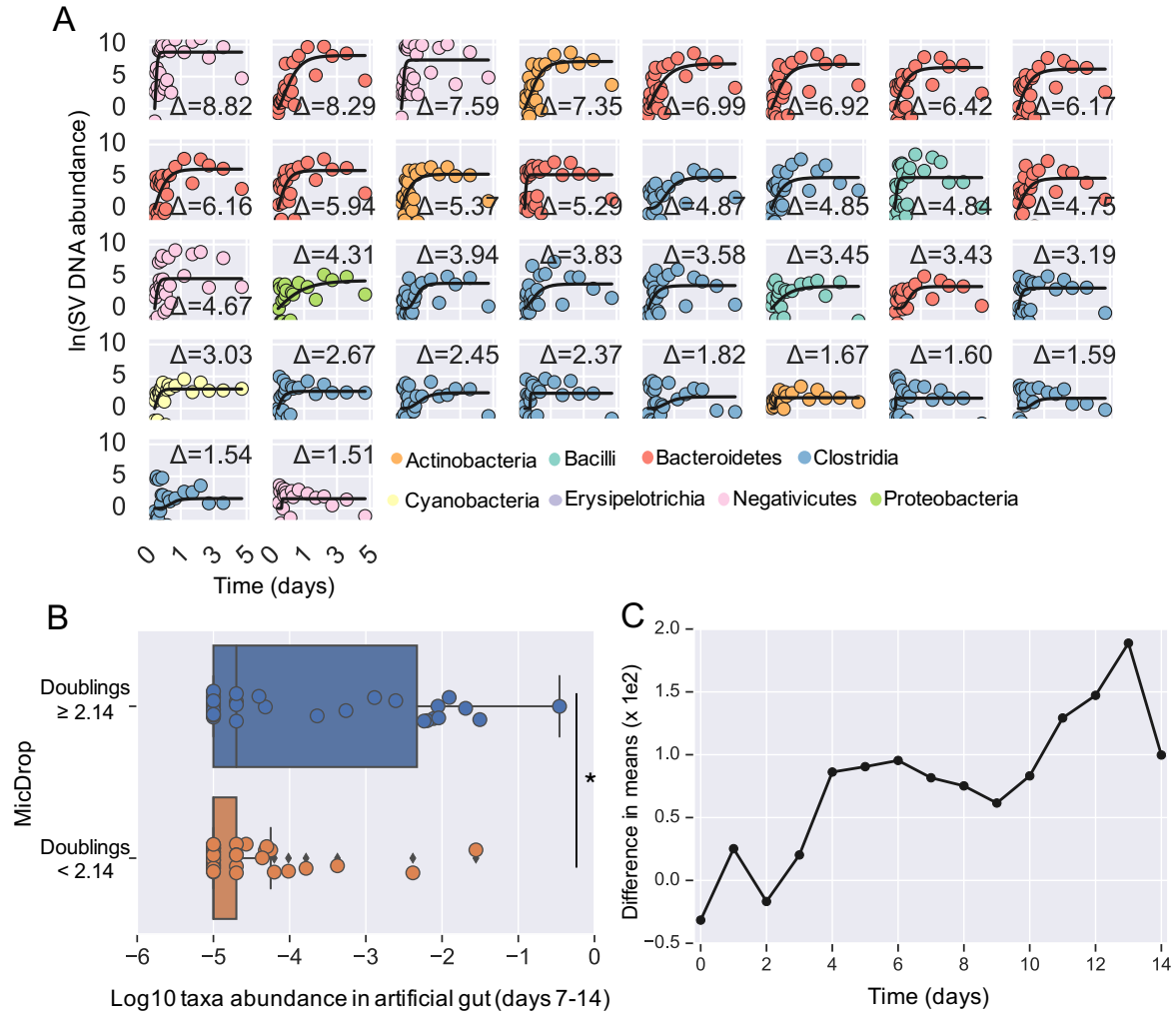

Figure 4. Comparison of SV growth kinetics and persistence in an artificial gut. (A) Abundance over time of SVs in MicDrop from a fresh human fecal sample. Modified Gompertz growth curves are fit to time-series. SVs are colored by taxonomy and sorted according to total growth (curve asymptote height; indicated by Δ), which is denoted on each sub-plot. Only SVs inferred to double at least 2.14 times were considering growing and are shown (ln(Δ SV DNA abundance) ≥1.48; threshold determined using control experiments in Supplementary Fig. 8). To ease viewing, curves are shifted vertically so y-intercepts are at the origin. (B) Long-term abundance of SVs in an artificial gut (grouped across days 7-14) grouped by whether SVs were identified by MicDrop as growing (doubling ≥ 2.14 times) or non-growing doubling < 2.14 times) (Mann-Whitney U, $p < 0.02$). (C) Differences in mean abundances of growing and non-growing SVs increased over time in an artificial gut system ($\rho=0.80$, $p < 0.0004$, Spearman correlation).

313 The growth of SVs measured with MicDrop were ultimately associated with SV
314 dynamics in the artificial gut. Such associations were not apparent on short-time scales
315 (i.e. 1-5 days after inoculation), which is consistent with the notion that non-growing SVs
316 require several days to wash out of an artificial gut after inoculation. However, from day
317 7-14 of the artificial gut experiment, we observed elevated abundances among artificial
318 gut SVs that grew in the MicDrop platform (inferred doublings ≥ 2.14) relative to ones
319 that did not (SV doublings < 2.14) (p < 0.02, Mann-Whitney U test) (Fig. 4B). This
320 difference in abundance increased over time in the artificial gut system (ρ = 0.80, p <
321 1e-4, Spearman correlation) (Fig. 4C). Still, some SVs grew well in droplets, but did not
322 persist in the artificial gut (left-most points of upper bar in Fig. 4B); or, by contrast, did
323 not grow in droplets, but were relatively abundant in the artificial gut (right-most points of
324 lower bar in Fig. 4B). The former may represent examples of SVs that are outcompeted
325 in mixed culture, while the latter may be examples of SVs that depend on inter-species
326 interactions to persist.
327
328 **Discussion**
329 We report here a microfluidic platform for isolating, culturing, and assaying
330 component members of human gut microbiota (MicDrop) using accessible microfluidic
331 and molecular techniques. We used MicDrop to compare the growth kinetics of dozens
332 of microbial SVs to the dynamics of an artificial gut community and to examine inter-
333 individual variation in gut bacterial polysaccharide metabolism. The flexibility of the
334 platform suggests its underlying concepts could be applied to assaying microbial
335 responses to other compounds including pharmaceuticals, antibiotics, or host-secreted

compounds[18,61] using individual members of communities comprised of microbes from culture collections, mutant libraries, other human body sites, or environmental systems. The ability of MicDrop to screen clonal populations could be particularly useful for assays characterizing the behavior of isolates free from the effects of inter-species interactions like competition or facilitation[17,18].

Yet, we acknowledge MicDrop still has some limitations. We rely on 16S rRNA as a molecular barcode for droplets sharing the same bacterial SV, meaning that the platform is sensitive to similar challenges due to inter-species rRNA copy number variation confronting 16S rRNA microbiota surveys[62]; and MicDrop cannot detect differences in growth originating from distinct clones of the same SV. For precise growth assays targeting bacteria from a limited number of taxa, traditional culture methods could be better suited. An additional limitation of MicDrop in its current form is the time and manual effort needed to setup individual droplet generation experiments and ensure accurate Poisson dilution of bacterial cells. Experimental effort could be reduced and reproducibility enhanced by automating sample switching. Last, we focused here on culture in liquid media using soluble substrates; future extensions of MicDrop that provide solid physical surfaces to colonize[63,64] or insoluble substrates like mucin will require developing techniques to avoid the clogging of microfluidic channels.

Still, in its present form, MicDrop enabled useful insights into human gut microbiology. Our findings that bacterial SV growth in isolation is associated with persistence in an artificial gut supports the ecological hypotheses that intrinsic lifestyle characteristics of bacteria shape overall community dynamics. Indeed, species' growth rate (measured by 16S rRNA copy number) is positively correlated with microbes'

359 relative abundance in seawater[65], as well as skin microbiota of amphibians[66].
360 Additionally, our microfluidic investigation of prebiotic response supports hypotheses
361 that inter-individual variation to carbohydrate interventions is due to differential
362 abundances of polysaccharide degrading bacteria between people[43,67]. Droplet
363 microfluidics could be used in the future to stratify human populations into groups most
364 likely to benefit from prebiotic treatments[41], by providing a culture-based diagnostic
365 approach capable of scaling to the diversity of microbes inhabiting the human gut.
366

References

1. Kendall, A.I. Some observations on the study of the intestinal bacteria. *Journal of Biological Chemistry* **6**, 499-507 (1909).
2. Rajilic-Stojanovic, M. & de Vos, W.M. The first 1000 cultured species of the human gastrointestinal microbiota. *FEMS microbiology reviews* **38**, 996-1047 (2014).
3. Le Barz, M. et al. In vivo screening of multiple bacterial strains identifies Lactobacillus rhamnosus Lb102 and Bifidobacterium animalis ssp. lactis Bf141 as probiotics that improve metabolic disorders in a mouse model of obesity. *FASEB journal : official publication of the Federation of American Societies for Experimental Biology* **4**, 4921-4935 (2018).
4. Zegarra-Ruiz, D.F. et al. A Diet-Sensitive Commensal Lactobacillus Strain Mediates TLR7-Dependent Systemic Autoimmunity. *Cell host & microbe* (2018).
5. Mathewson, N.D. et al. Gut microbiome-derived metabolites modulate intestinal epithelial cell damage and mitigate graft-versus-host disease. *Nature immunology* **17**, 505-513 (2016).
6. Larsbrink, J. et al. A discrete genetic locus confers xyloglucan metabolism in select human gut Bacteroidetes. *Nature* **506**, 498-502 (2014).
7. Whiteside, S.A., Razvi, H., Dave, S., Reid, G. & Burton, J.P. The microbiome of the urinary tract--a role beyond infection. *Nat Rev Urol* **12**, 81-90 (2015).
8. Buffie, C.G. et al. Precision microbiome reconstitution restores bile acid mediated resistance to Clostridium difficile. *Nature* (2014).
9. Routy, B. et al. The gut microbiota influences anticancer immunosurveillance and general health. *Nat Rev Clin Oncol* **15**, 382-396 (2018).
10. Eckburg, P.B. et al. Diversity of the human intestinal microbial flora. *Science* **308**, 1635-1638 (2005).
11. Human Microbiome Project, C. Structure, function and diversity of the healthy human microbiome. *Nature* **486**, 207-214 (2012).
12. Yatsunenko, T. et al. Human gut microbiome viewed across age and geography. *Nature* **486**, 222-227 (2012).
13. De Filippo, C. et al. Impact of diet in shaping gut microbiota revealed by a comparative study in children from Europe and rural Africa. *Proceedings of the National Academy of Sciences of the United States of America* **107**, 14691-14696 (2010).
14. Faith, J.J. et al. The long-term stability of the human gut microbiota. *Science* **341**, 1237439 (2013).
15. Goodman, A.L. et al. Extensive personal human gut microbiota culture collections characterized and manipulated in gnotobiotic mice. *Proceedings of the National Academy of Sciences of the United States of America* **108**, 6252-6257 (2011).
16. Lagier, J.C. et al. The rebirth of culture in microbiology through the example of culturomics to study human gut microbiota. *Clinical microbiology reviews* **28**, 237-264 (2015).

17. Desai, M.S. et al. A Dietary Fiber-Deprived Gut Microbiota Degrades the Colonic Mucus Barrier and Enhances Pathogen Susceptibility. *Cell* **167**, 1339-1353 (2016).
18. Maier, L. et al. Extensive impact of non-antibiotic drugs on human gut bacteria. *Nature* **555**, 623-628 (2018).
19. Martin, K. et al. Generation of larger numbers of separated microbial populations by cultivation in segmented-flow microdevices. *Lab on a chip* **3**, 202-207 (2003).
20. Ma, L. et al. Gene-targeted microfluidic cultivation validated by isolation of a gut bacterium listed in Human Microbiome Project's Most Wanted taxa. *Proceedings of the National Academy of Sciences of the United States of America* **111**, 9768-9773 (2014).
21. Nichols, D. et al. Use of ichip for high-throughput in situ cultivation of "uncultivable" microbial species. *Applied and environmental microbiology* **76**, 2445-2450 (2010).
22. Kaminski, T.S., Scheler, O. & Garstecki, P. Droplet microfluidics for microbiology: techniques, applications and challenges. *Lab on a chip* **16**, 2168-2187 (2016).
23. Guo, M.T., Rotem, A., Heyman, J.A. & Weitz, D.A. Droplet microfluidics for high-throughput biological assays. *Lab on a chip* **12**, 2146-2155 (2012).
24. Zengler, K. et al. Cultivating the uncultured. *Proceedings of the National Academy of Sciences of the United States of America* **99**, 15681-15686 (2002).
25. Liu, W., Kim, H.J., Lucchetta, E.M., Du, W. & Ismagilov, R.F. Isolation, incubation, and parallel functional testing and identification by FISH of rare microbial single-copy cells from multi-species mixtures using the combination of chemistrode and stochastic confinement. *Lab on a chip* **9**, 2153-2162 (2009).
26. Park, J., Kerner, A., Burns, M.A. & Lin, X.N. Microdroplet-enabled highly parallel co-cultivation of microbial communities. *PloS one* **6**, e17019 (2011).
27. Huang, S. et al. Dynamic control and quantification of bacterial population dynamics in droplets. *Biomaterials* **61**, 239-245 (2015).
28. Terekhov, S.S. et al. Ultrahigh-throughput functional profiling of microbiota communities. *Proceedings of the National Academy of Sciences of the United States of America* **115**, 9551-9556 (2018).
29. Terekhov, S.S. et al. Microfluidic droplet platform for ultrahigh-throughput single-cell screening of biodiversity. *Proceedings of the National Academy of Sciences of the United States of America* **114**, 2550-2555 (2017).
30. Browne, H.P. et al. Culturing of 'unculturable' human microbiota reveals novel taxa and extensive sporulation. *Nature* **533**, 543-546 (2016).
31. Callahan, B.J. et al. DADA2: High-resolution sample inference from Illumina amplicon data. *Nature methods* **13**, 581-583 (2016).
32. Najah, M., Griffiths, A.D. & Ryckelynck, M. Teaching single-cell digital analysis using droplet-based microfluidics. *Analytical chemistry* **84**, 1202-1209 (2012).
33. Martens, E.C., Chiang, H.C. & Gordon, J.I. Mucosal glycan foraging enhances fitness and transmission of a saccharolytic human gut bacterial symbiont. *Cell host & microbe* **4**, 447-457 (2008).
34. El Kaoutari, A., Armougom, F., Gordon, J.I., Raoult, D. & Henrissat, B. The abundance and variety of carbohydrate-active enzymes in the human gut microbiota. *Nature Reviews Microbiology* **11**, 497-504 (2013).

35. Ze, X., Duncan, S.H., Louis, P. & Flint, H.J. Ruminococcus bromii is a keystone species for the degradation of resistant starch in the human colon. *The ISME journal* **6**, 1535 (2012).
36. Slavin, J. Fiber and Prebiotics: Mechanisms and Health Benefits. *Nutrients* **5**, 1417-1435 (2013).
37. Kamada, N. et al. Regulated virulence controls the ability of a pathogen to compete with the gut microbiota. *Science* **336**, 1325-1329 (2012).
38. Rakoff-Nahoum, S., Coyne, M.J. & Comstock, L.E. An ecological network of polysaccharide utilization among human intestinal symbionts. *Current biology : CB* **24**, 40-49 (2014).
39. Furusawa, Y. et al. Commensal microbe-derived butyrate induces the differentiation of colonic regulatory T cells. *Nature* **504**, 446-450 (2013).
40. Makki, K., Deehan, E.C., Walter, J. & Backhed, F. The Impact of Dietary Fiber on Gut Microbiota in Host Health and Disease. *Cell host & microbe* **23**, 705-715 (2018).
41. Venkataraman, A. et al. Variable responses of human microbiomes to dietary supplementation with resistant starch. *Microbiome* **4** (2016).
42. Martinez, I., Kim, J., Duffy, P.R., Schlegel, V.L. & Walter, J. Resistant Starches Types 2 and 4 Have Differential Effects on the Composition of the Fecal Microbiota in Human Subjects. *PloS one* **5** (2010).
43. Walker, A.W. et al. Dominant and diet-responsive groups of bacteria within the human colonic microbiota. *Isme Journal* **5**, 220-230 (2011).
44. Chu, N.D., Smith, M.B., Perrotta, A.R., Kassam, Z. & Alm, E.J. Profiling Living Bacteria Informs Preparation of Fecal Microbiota Transplantations. *PloS one* **12**, e0170922 (2017).
45. Magnusdottir, S. et al. Generation of genome-scale metabolic reconstructions for 773 members of the human gut microbiota. *Nature biotechnology* **35**, 81-89 (2017).
46. Noronha, A. et al. The Virtual Metabolic Human database: integrating human and gut microbiome metabolism with nutrition and disease. *Nucleic acids research* **47**, D614-D624 (2019).
47. Newton, D.F., Macfarlane, S. & Macfarlane, G.T. Effects of antibiotics on bacterial species composition and metabolic activities in chemostats containing defined populations of human gut microorganisms. *Antimicrobial agents and chemotherapy* **57**, 2016-2025 (2013).
48. Gamage, H. et al. Cereal products derived from wheat, sorghum, rice and oats alter the infant gut microbiota in vitro. *Scientific reports* **7**, 14312 (2017).
49. Ichim, T.E., Kesari, S. & Shafer, K. Protection from chemotherapy- and antibiotic-mediated dysbiosis of the gut microbiota by a probiotic with digestive enzymes supplement. *Oncotarget* **9**, 30919-30935 (2018).
50. Rajilic-Stojanovic, M. et al. Evaluating the microbial diversity of an in vitro model of the human large intestine by phylogenetic microarray analysis. *Microbiology* **156**, 3270-3281 (2010).
51. McDonald, J.A. et al. Evaluation of microbial community reproducibility, stability and composition in a human distal gut chemostat model. *J Microbiol Methods* **95**, 167-174 (2013).

52. Van den Abbeele, P. et al. Microbial Community Development in a Dynamic Gut Model Is Reproducible, Colon Region Specific, and Selective for Bacteroidetes and Clostridium Cluster IX. *Applied and environmental microbiology* **76**, 5237-5246 (2010).
53. Auchtung, J.M., Robinson, C.D. & Britton, R.A. Cultivation of stable, reproducible microbial communities from different fecal donors using minibioreactor arrays (MBRAs). *Microbiome* **3**, 42 (2015).
54. Tramontano, M. et al. Nutritional preferences of human gut bacteria reveal their metabolic idiosyncrasies. *Nat Microbiol* **3**, 514-522 (2018).
55. Freeman, J., O'Neill, F.J. & Wilcox, M.H. Effects of cefotaxime and desacetylcefotaxime upon Clostridium difficile proliferation and toxin production in a triple-stage chemostat model of the human gut. *J Antimicrob Chemoth* **52**, 96-102 (2003).
56. Macfarlane, G.T., Macfarlane, S. & Gibson, G.R. Validation of a Three-Stage Compound Continuous Culture System for Investigating the Effect of Retention Time on the Ecology and Metabolism of Bacteria in the Human Colon. *Microbial ecology* **35**, 180-187 (1998).
57. Silverman, J.D., Durand, H.K., Bloom, R.J., Mukherjee, S. & David, L.A. Dynamic linear models guide design and analysis of microbiota studies within artificial human guts. *Microbiome* **6**, 202 (2018).
58. Reese, A.T. et al. Antibiotic-induced changes in the microbiota disrupt redox dynamics in the gut. *eLife* **7** (2018).
59. Rettedal, E.A., Gumpert, H. & Sommer, M.O. Cultivation-based multiplex phenotyping of human gut microbiota allows targeted recovery of previously uncultured bacteria. *Nat Commun* **5**, 4714 (2014).
60. Lagier, J.C. et al. Microbial culturomics: paradigm shift in the human gut microbiome study. *Clinical microbiology and infection : the official publication of the European Society of Clinical Microbiology and Infectious Diseases* **18**, 1185-1193 (2012).
61. Koppel, N., Maini Rekdal, V. & Balskus, E.P. Chemical transformation of xenobiotics by the human gut microbiota. *Science* **356** (2017).
62. Kembel, S.W., Wu, M., Eisen, J.A. & Green, J.L. Incorporating 16S gene copy number information improves estimates of microbial diversity and abundance. *PLoS computational biology* **8**, e1002743 (2012).
63. Macfarlane, S., Woodmansey, E.J. & Macfarlane, G.T. Colonization of mucin by human intestinal bacteria and establishment of biofilm communities in a two-stage continuous culture system. *Applied and environmental microbiology* **71**, 7483-7492 (2005).
64. Datta, M.S., Sliwerska, E., Gore, J., Polz, M.F. & Cordero, O.X. Microbial interactions lead to rapid micro-scale successions on model marine particles. *Nature communications* **7**, 11965 (2016).
65. Campbell, B.J. & Kirchman, D.L. Bacterial diversity, community structure and potential growth rates along an estuarine salinity gradient. *The ISME journal* **7**, 210-220 (2013).

66. Prest, T.L., Kimball, A.K., Kueneman, J.G. & McKenzie, V.J. Host-associated bacterial community succession during amphibian development. *Molecular ecology* **27**, 1992-2006 (2018).
67. Kovatcheva-Datchary, P. et al. Dietary Fiber-Induced Improvement in Glucose Metabolism Is Associated with Increased Abundance of Prevotella. *Cell Metabolism* **22**, 971-982 (2015).
68. Caporaso, J.G. et al. Global patterns of 16S rRNA diversity at a depth of millions of sequences per sample. *Proceedings of the National Academy of Sciences of the United States of America* **108**, 4516-4522 (2011).
69. Maurice, C.F., Haiser, H.J. & Turnbaugh, P.J. Xenobiotics shape the physiology and gene expression of the active human gut microbiome. *Cell* **152**, 39-50 (2013).
70. Caporaso, J.G. et al. QIIME allows analysis of high-throughput community sequencing data. *Nat Methods* **7**, 335-336 (2010).
71. Wang, Q., Garrity, G.M., Tiedje, J.M. & Cole, J.R. Naive Bayesian classifier for rapid assignment of rRNA sequences into the new bacterial taxonomy. *Applied and environmental microbiology* **73**, 5261-5267 (2007).
72. Quast, C. et al. The SILVA ribosomal RNA gene database project: improved data processing and web-based tools. *Nucleic acids research* **41**, D590-D596 (2013).
73. Zwietering, M.H., Jongenburger, I., Rombouts, F.M. & van 't Riet, K. Modeling of the bacterial growth curve. *Applied and environmental microbiology* **56**, 1875-1881 (1990).
74. Sottile, W., 2nd & Zabransky, R.J. Comparative growth rates of selected anaerobic species in four commonly used broth media. *Antimicrobial agents and chemotherapy* **11**, 482-490 (1977).
75. Monod, J. The Growth of Bacterial Cultures. *Annual review of microbiology* **3**, 371-394 (1949).
76. Reese, A.T. et al. Microbial nitrogen limitation in the mammalian large intestine. *Nat Microbiol* **3**, 1441-1450 (2018).
77. Bochner, B.R., Gadzinski, P., & Panomitros E. Phenotype microarrays for high-throughput phenotypic testing and assay of gene function. *Genome Research* **11**, 1246-1255 (2001)
78. Magnúsdóttir, S. et al. Generation of genome-scale metabolic reconstructions for 773 members of the human gut microbiota. *Nature Biotechnology*, 81-89 (2017).

EXPERIMENTAL PROCEDURES

Overall MicDrop procedure

Droplets were made on a microfluidic chip (6-junction droplet chip, Dolomite Microfluidics). Bacterial media varied by assay; for the oil phase, we used a fluorinated oil and surfactant mixture 1% Picosurf (Sphere Fluidics) in Novec 7500 (3M). One day

prior to performing the droplet assay, all reagents including carrier oil, culture media, and carbon solutions were equilibrated to the anaerobic atmosphere in an anaerobic chamber (Coy). The fecal inoculum optical density at 600 nm was recorded and diluted according to the Poisson distribution: $P(n,\bar{n}) = \frac{\bar{n}^n e^{-\bar{n}}}{n!}$, where n is the droplet occupancy (i.e. 0,1,.. cells/droplet) and $\bar{n}$ is the average number of cells per droplet given by: $\bar{n} = \rho V$, where V is droplet volume and ρ is cell density. Assays were performed at a $\bar{n}$ of 0.1-0.3 to minimize the number of droplets loaded with more than one cell (Supplementary Fig. 1). Thus, for a fixed droplet volume and $\bar{n}$, the target cell concentration can be obtained from: $\rho = K\frac{\bar{n}}{V}$, where *K* is a constant that converts CFUs/mL to OD_{600} determined from replicate CFU assays. Syringe pumps were used to control the flow rates of the oil and cell suspension (NE-1000 Single Syringe Pump, New Era Pump Systems). Following the culture period, droplets were loaded into chambered slides (C10283, Invitrogen) or directly onto glass slides and observed with Phase and/or Darkfield microscopy (Nikon) to examine growth and the appropriate loading. All steps of cell encapsulation and culture were performed in an anaerobic chamber.

Collection and preparation of fecal inoculum for artificial gut and MicDrop growth dynamics assays

Stool was collected from human donors under a protocol approved by the Duke Health Institutional Review Board (Duke Health IRB Pro00049498). Inclusion criteria limited this study to healthy subjects who could provide fecal samples at no risk to themselves, had no acute enteric illness (e.g. diarrhea) and had not taken antibiotics in

611 the past month. Fresh stool samples were collected in a disposable commode specimen
612 container (Fisher Scientific, Hampton NH). Intact stool was moved within roughly 15
613 minutes of bowel movement into anaerobic conditions. The sample was prepared for
614 inoculation in an anaerobic chamber (Coy). A 5 g stool aliquot was weighed into a 7 oz
615 filtration bag (Nasco Whirl-Pak) and combined with 50 mL of mGAM media (Gifu
616 Anaerobic Medium, HiMedia, with the addition of 5 mg/L Vitamin K and 10 mg/L Hemin,
617 [59]) that was pre-reduced overnight in an anaerobic chamber. The mixture was
618 homogenized in a stomacher (Seward Stomacher 80) on normal speed for 1 minute
619 under atmospheric conditions to make a total of 100 mL of inoculum. The supernatant
620 was decanted into beakers and loaded into syringes for inoculation into the artificial gut
621 or filtered through a 50 μm filter (Celltrics) and diluted and loaded into droplets.
622
623 **Droplet DNA extraction, PCR amplification, and DNA sequencing**
624 To extract DNA from droplets, excess oil was removed by pipetting and water-in-
625 oil emulsions were broken by adding an equal amount of 1H,1H,2H,2H-Perfluoro-1-
626 octanol (PFO, VWR) and briefly vortexed. Then, the samples were briefly centrifuged
627 (<200 g) to separate the aqueous and oil phases by density. The aqueous solution was
628 transferred to a new tube, and DNA was extracted using a kit (Qiagen #12224). DNA
629 was extracted from artificial gut and stool samples using a 96-well PowerSoil kit (Qiagen
630 #12888). For all samples, the V4 region of the 16S rRNA gene was barcoded and
631 amplified from extracted DNA using with custom barcoded primers, using published
632 protocols[68,69]. 16S rRNA amplicon sequencing was performed on an Illumina MiniSeq
633 with paired-end 150 bp reads. We chose to only analyze samples with more than 5,000

reads to remove outlying samples that may have been subject to library preparation or sequencing artifacts. The 16S rRNA nucleotide sequences generated in this study will be made available at the European Nucleotide Archive under study accession number TBD. Total bacterial abundances from droplet cultures were estimated by qPCR for bacterial 16S rRNA using the same primers used in the DNA sequencing protocol. Amplification during the qPCR process was measured with a Real-Time PCR system (CFX96 Real-Time System, BioRad) using *E. coli* DNA at a known cell concentration as a reference.

Identifying Sequence Variants and Taxonomy assignment

DADA2 was used to identify SVs[31]. Custom scripts were used to prepare data for denoising with DADA2 as previously described[57]. Reads were then demultiplexed using scripts in Qiime v1.9[70]. SVs were inferred by DADA2 using error profiles learned from a random subset of 40 samples from each sequencing run. Bimeras were removed using the function removeBimeraDenovo with tableMethod set to “consensus”. Taxonomy was assigned to sequence variants using a Naïve Bayes classifier[71] trained using version 123 of the SILVA database[72]. For growth dynamics of the human gut microbiota and microbiota dynamics in the artificial gut, only forward sequencing reads were analyzed. Downstream analysis on sequence variant tables was performed using R (ver. 3.4.2) and Python (ver. 2.7.6). PERMANOVA was run in R using adonis in the vegan package (ver. 2.5-2).

Growth dynamics of human gut microbiota

To estimate SV growth curves using MicDrop, we collected a total of 70 separate microfluidic droplet aliquots for destructive longitudinal sampling. Droplets were generated according to the MicDrop protocol described above. We used a modified Gifu Anaerobic Medium (mGAM) in our droplets (Gifu Anaerobic Medium, HiMedia, with the addition of 5 mg/L Vitamin K and 10 mg/L Hemin). Each aliquot of 200 µl of droplets was incubated at 37 °C in an anaerobic chamber. Aliquots were destructively sampled in triplicate, hourly, for hours 0-24 after droplet making and in duplicate once a day for hours 24-127 after droplet making.

Growth curves were fit using a combination of 16S rRNA qPCR and DNA sequencing data. To minimize the potential for poorly fit growth curves, SVs were required to have been detected by DNA sequencing in >5 samples to be included in curve fitting. To avoid numerical instabilities associated with taking the log or dividing by zero, a pseudocount of one was added to the sequence variant count table prior to normalization to relative abundances. Relative abundances of each SV were then determined by dividing the number of counts associated with each SV in each sample by the total read counts in the sample. Concentrations of each taxa were then estimated by multiplying the relative abundances of SVs by the 16S rRNA concentrations determined by qPCR. Technical replicates constituted distinct data points in these calculations. We used the SciPy Python package (v0.19.1) to fit a modified Gompertz equation[73] to which we added an additional term to account for differences in starting abundance to the resulting dataset: $y = Aexp\left\{-exp\left[\frac{\mu \cdot e}{A}(\lambda - t) + 1\right]\right\} + A_0$, where µ is growth rate, A is carrying capacity, λ is lag time, or the time it takes for a bacteria to reach logarithmic growth, and A_0 accounts for the relative abundance of different SVs in

680 the inoculum. We fit curves using the module scipy.optimize.least_squares with the
681 robust loss function “soft_l1”. Parameter bounds were also used to minimize the
682 optimization search space. We set lower bounds of A=0, λ=-50, μ=0, A_0=0; and, upper
683 bounds of *A*=15, λ=12, μ=2.6, A_0=15. We selected bounds by considering both
684 biological feasibility and parameter sensitivity analyses (Supplementary Fig. 12). Our
685 upper bound for growth rate (μ=2.6) represented a doubling time of 15 minutes, which
686 we based on the fastest growth rates observed in an anaerobic bacterium[74]. The upper
687 bounds on *A* and A_0 were set to the maximum amount of DNA measured across
688 replicate MicDrop samples from the human fecal inoculum. The upper bound on λ,
689 which represents the lag time until exponential growth[75] was set at 12. Lower bounds of
690 0 for *A*, A_0, and μ reflect our choice not to model negative growth. A lower bound for λ
691 was selected by sensitivity analysis (Supplementary Fig. 12), which revealed that a
692 bound of zero led to fitted λ values regularly collapsing to our boundary limits. We also
693 found that fitted curves were sensitive to starting parameters. To ensure a broad search
694 of parameter space, we initialized each curve fit multiple times (n=100) with starting
695 parameters randomly distributed between the bounds of each parameter. Fitted growth
696 rates often collapsed to the maximum μ tolerated; we therefore only retained fits where
697 growth rates were at least slightly below our upper bound for μ (μ < 2.5) (Supplementary
698 Fig. 13). Of the remaining fitted curves, we analyzed the one with the lowest loss
699 function. In our analyses of SV growth in human fecal samples, we defined total SV
700 levels as *y*(127 hours) - *y*(0 hours).
701
702 **Microbiota dynamics in an artificial human gut**

We cultured human gut microbiota with an artificial gut model that we have used in prior studies[57,76]. A continuous-flow artificial gut system (Multifors 2, Infors) was used to culture gut microbiota seeded from human stool. A vessel was autoclave-sterilized and prepared with 300 mL of mGAM media (see *Growth dynamics of human gut microbiota* above). We inoculated the vessel with 100 mL of fecal inoculum, resulting in a total culture volume of 400 mL. After 24 hours, the media feed was initiated at a constant rate of 400 mL per day. A carboy feeding the media was changed once over the course of the 14 days. Feed rate, oxygen, pH, temperature, and stir rate were all controlled by software (IRIS v6, Infors). Positive pressure within the vessels was maintained to prevent contamination by sparging with nitrogen at 1 LPM. Dissolved oxygen concentration was measured continuously using Hamilton VisiFerm DO Arc 225 probes. pH was monitored with Hamilton EasyFerm Plus PH ARC 225 probes and was maintained between 6.9 and 7.1 using a 1 N HCl solution and a 1 N H_3PO_4 solution. The vessel was maintained at 37°C via the Infors' onboard temperature control system. The vessel was continuously stirred at 100 rpm using magnetic impeller stir-shafts. Samples were taken once every 24 hours between 1 PM and 5 PM for 14 days and were frozen immediately at -80°C for later extraction.

MicDrop Prebiotic Assay

Microbial communities isolated from human stool samples were tested for carbohydrate consumption using the MicDrop platform. Cells were revived from frozen stock in rich medium (mGAM, see *Growth dynamics of human gut microbiota*) for 18 hours to allow cells to recover from freezing. Bacteria were then cultured in minimal medium

(Supplementary Table 6) containing glucose and galactose (Sigma) as the sole carbon sources to deplete excess nutrients[77]. Following determination of the loading concentration, the bacteria were washed twice by centrifugation (2 min at 14,000 g) to remove free monosaccharides and resuspended in 2X minimal medium without a carbon source. Bacteria were filtered using a 50 µm filter (CellTrics, Sysmex) to remove multi-cell clumps. The filtered microbiota suspension was then added to prebiotics in a 50:50 mixture of 1% prebiotic solution and 2X minimal medium. To prevent chip fouling during droplet generation, the oil inlet was equipped with 10 µm inline filters (P-276, IDEX). Droplet generation in the anaerobic chamber was monitored using a bright field microscope (Celestron). Droplet cultures were stored in 5 mL polypropylene tubes (Falcon) with the caps closed in an anaerobic incubator at 37 °C. Following the second day of incubation, cultures were moved to a -20 °C freezer for storage prior to DNA extraction.

Validation of prebiotic utilization assays

To validate the MicDrop prebiotic assay, we generated reference data on carbohydrate preferences using an artificial community of seven wild-type gut isolates from our culture collection (Supplementary Table 7), which were grown in both 96-well plates and the MicDrop Prebiotic Assay described in the preceding paragraph. Following the same procedure described in the *MicDrop Prebiotic Assay*, well plates were prepared with minimal medium (Supplementary Table 6) and a carbohydrate as a sole carbon source (Supplementary Table 8). A 10 µL aliquot of bacterial suspension was added to 200 µL of medium in 96-well plates and incubated in a humidified container for two days at 37

749 °C. All culture experiments were performed in an anaerobic chamber. Following the
750 culture period, the optical density at 600 nm of each well was examined using a plate
751 reader (CLARIOstar, BMG Labtech). Following published protocols[17], isolate growth in
752 plates was normalized to the maximum growth for each microbe. To classify isolates as
753 either “growing” or “not-growing,” a threshold of 20% of maximum growth was applied to
754 the plate data, above which was considered growth on the carbon source of interest.
755 The same isolates used in the well-plate analyses were mixed evenly into an artificial
756 community and examined using the MicDrop prebiotic assay described above. MicDrop
757 experiments were performed in triplicate. Growth thresholds for the MicDrop assay were
758 determined by first pre-processing sample qPCR values to zero if they indicated overall
759 growth below mean no-carbon controls. Then, relative SV abundance data were
760 converted to absolute SV abundances by multiplying each sample by the corresponding
761 qPCR value. Median SV abundances were then calculated across replicates and SV
762 abundances from matched no-carbon controls were subtracted from each sample. An
763 optimal SV growth threshold for determining growth on a carbohydrate in MicDrop was
764 determined by applying Youden’s J index across all possible threshold values, with the
765 well-plate data as the reference (Supplementary Fig. 9). A growth threshold of 88%
766 maximized this index and was used in subsequent experiments on fecal samples.
767
768 **MicDrop prebiotic assays using human stool samples**
769 Stool samples were collected from nine healthy donors (7 men, 2 women) between the
770 ages of 35-53 under the IRB protocol described in section *Collection and preparation of*
771 *fecal inoculum for artificial gut and MicDrop growth dynamics assays*. To facilitate

carrying out prebiotic assays simultaneously across a range of donors, we used frozen gut microbiota in these experiments. Fecal slurries were made at 10% w/v using mGAM medium and a stomacher (Seward) that homogenized fecal samples for one minute. Then, slurries were mixed 50:50 with 50% glycerol and stored at -80 °C for later use. Samples were assayed following the MicDrop prebiotic assay procedure described above.

Comparison of primary degraders to the Virtual Metabolic Human database

We compared the identity of primary degraders to carbon consumption profiles from the Virtual Metabolic Human (VMH) database[46,78]. We first mapped primary degraders to this database by taking SV 16S rRNA sequences from our study and searching for matches in the NCBI nucleotide database. Each 100% match was then linked to a type strain in the VMH database using NCBI taxonomy ids. Since some NCBI taxonomy IDs could be mapped to multiple strain IDs, we used an NCBI genome assembly file (ftp://ftp.ncbi.nlm.nih.gov/genomes/ASSEMBLY_REPORTS/assembly_summary_genbank.txt) to perform more specific mappings; when more than one mapping was possible, we selected the strain with the oldest genome annotation (we reasoned that strains that were selected first for sequencing were also more likely to have more thorough experimental characterizations). Once SVs were mapped, we restricted our analysis to SVs that grew on a given carbohydrate in over half of the participants and where all BLAST matches to the VMH database had concordant prebiotic utilization annotations. Only consumption of xylan and inulin were examined since GOS and dextrin were not referenced in the VMH database. Permutation analysis

795 were carried out by randomly shuffling rows and columns of the droplet primary
796 degrader table and repeating the analyses.
797
798
799 **Acknowledgements**
800 The authors would like to thank Christopher Mancuso and Ahmad S. Khalil, Ph.D., for
801 their helpful comments on the manuscript. L.A.D. acknowledges support from the
802 Global Probiotics Council, a Searle Scholars Award, an Alfred P. Sloan Research
803 Fellowship, the Beckman Young Investigator program, the Translational Research
804 Institute through Cooperative Agreement NNX16AO69A, the Damon Runyon Cancer
805 Research Foundation, the UNC CGIBD (NIDDK P30DK034987), and NIH
806 1R01DK116187-01. This work used a high-performance computing facility partially
807 supported by grant 2016-IDG-1013 (“HARDAC+: Reproducible HPC for Next-
808 generation Genomics") from the North Carolina Biotechnology Center. *E. coli* strain
809 was provided by N. Lord and J. Paulsson. M.M.V. holds a Postdoctoral Enrichment
810 Program Award from the Burroughs Wellcome Fund. This material is based upon work
811 supported by the National Science Foundation Graduate Research Fellowship under
812 Grant No. DGE-1644868 to R.J.B.
813
814 **Author contributions**
815 M.M.V., R.J.B., and L.A.D. developed the assay platform and designed the study.
816 M.M.V., R.J.B., H.K.D, S.H., S.J. and A.W. performed the experiments. J.D.S.
817 contributed software for bioinformatic analysis. M.M.V., R.J.B., and L.A.D. analyzed the

818 data. S.H. and L.Y. helped with design and data interpretation. M.M.V., R.J.B., and
819 L.A.D. wrote the manuscript with feedback from all authors.
820
821
822 **Competing interests**
823 M.M.V., R.J.B., L.A.D., and Duke University have patents filed related to the droplet
824 platform described herein (PCT/US20 17/045 608, 62/628 170). L.A.D. was a member
825 of the Kaleido Biosciences Strategic Advisory Board and retains equity in the company.